



Enhanced phosphorus regeneration linked to Ediacaran ocean oxygenation



Dongtao Xu ^{1,2,3}, Xinqiang Wang ^{1,2,3} , Eva E. Stüeken ⁴, Weiming Xu ^{5,6}, Zheng Qin ⁷, Jihua Hao ^{5,6}, Xiaoying Shi ^{1,2,3} & Dongjie Tang ^{1,2,8}

Several pulses of ocean oxygenation events were recognized in the Ediacaran period. However, the intrinsic triggers behind them remain ambiguous. Here we report phosphorus speciation data from the Ediacaran Doushantuo Formation, South China, to elucidate the role of recycled phosphorus in driving ocean oxygenation. High ratios of organic carbon to organic phosphorus in all samples relative to the Redfield ratio generally imply preferential release of phosphorus during the remineralization of organic matter. Notably, ratios of organic carbon to reactive phosphorus exceed the Redfield ratio during purported oxygenation intervals, but fall mostly below or close to the Redfield ratio in the rest of the section. Quantitative calculations suggest that enhanced benthic and water-column recycling created a phosphorus influx into the ocean that was comparable to or outpaced that of weathering input. Our study provides empirical evidence for untangling the mechanisms of the Ediacaran oxygenation.

Mounting evidence has demonstrated that the Earth's surface environment underwent several pulses of (if not permanent) oxygenation during the Ediacaran Period (ca. 635–538 Ma)^{1–3}. Although substantial uncertainties persist regarding atmospheric oxygen levels and the extent of ocean oxygenation, it is conceivable that a more oxygenated Earth, coupled with a sophisticated Ediacaran ecosystem⁴ was driven by elevated primary productivity, which, in turn, is dependent on marine nutrient levels.

Phosphorus (P) is widely regarded as the primary limiting nutrient modulating changes of primary productivity on geological timescales⁵. The principal source of dissolved P to the global ocean is riverine input from continental weathering^{6,7}. Enhanced continental chemical weathering would have increased bioavailable P in surface seawater, consequently fueling marine primary productivity^{8–10}. The removal of seawater P is mainly through organic matter burial and precipitation of Fe minerals in marine sediments^{6,7}. However, this drawdown of seawater P can be compensated by recycled P via remineralization of organic matter and reduction of Fe (oxyhydr)oxides in the water column and in sediments^{11–14}, driving further primary productivity. However, not all the regenerated P can be released to seawater to fuel primary productivity. Depending on the local redox conditions, some, or even all, of the recycled P may be re-trapped in the sediments through 'sink switching', forming authigenic apatite and/or Fe phosphates (for example, vivianite)^{13–17}. Hence, a detailed reconstruction of

the phosphorus cycle is key for understanding the nature and history of redox changes in Earth's surface environment.

Current geological and geochemical evidence, including the onset of massive phosphorite deposition¹⁸, bulk P content in shales^{19,20}, P/Fe ratios in ironstones^{9,21}, and carbonate-associated phosphate²², all suggest an elevated seawater P in the Ediacaran ocean. But the reason behind this increase is contentious. Some researchers propose that enhanced weathering following the termination of Cryogenian glaciations may have caused a large input of P into the earliest Ediacaran oceans, fueling primary productivity, organic matter burial and ocean oxygenation^{9,23}. However, this idea is challenged since a transient increase of riverine P input, even by a factor of two, can not easily match the time span and scale of massive Ediacaran phosphorites¹⁸. Alternatively, recycled P mobilized by bacterial sulfate reduction of organic matter has been suggested as the major source of elevated seawater P in Ediacaran oceans^{18,22,24–26}, but direct evidence for this argument is lacking. To elucidate the potential role of recycled P in sustaining high dissolved P levels and primary productivity, we performed analyses of the P speciation in the Ediacaran Doushantuo black shales collected from the well-preserved Wuhe section in South China. Our sample set covers an established perturbation in redox conditions, revealed by Fe speciation², molybdenum (Mo) and mercury (Hg) isotopes^{27,28}, enabling us to explore the connection between recycled P, primary productivity, and ocean oxygenation in the critical transition of Earth's history.

¹State Key Laboratory of Geomicrobiology and Environmental Changes, China University of Geosciences (Beijing), Beijing, China. ²Frontiers Science Center for Deep-time Digital Earth, China University of Geosciences (Beijing), Beijing, China. ³School of Earth Sciences and Resources, China University of Geosciences (Beijing), Beijing, China. ⁴School of Earth & Environmental Sciences, University of St Andrews, St Andrews, UK. ⁵CAS Key Laboratory of Crust-Mantle Materials and Environments, School of Earth and Space Sciences, University of Science and Technology of China, Hefei, China. ⁶CAS Center for Excellence in Comparative Planetology, University of Science and Technology of China, Hefei, China. ⁷State Key Laboratory of Geological Processes and Mineral Resources, China University of Geosciences, Beijing, China. ⁸Institute of Earth Sciences, China University of Geosciences (Beijing), Beijing, China. e-mail: wxqiang307@126.com

Sampling and results

The samples in this study were collected from the Ediacaran Doushantuo Formation (ca. 635–556 Ma) of the Wuhe section (GPS: 26°45'56" N, 108°25'01" E) in Jianhe County, Guizhou Province, South China (Fig. 1a, b). This section was deposited in a lower slope setting with good connection to the open ocean^{2,29}. The Doushantuo Formation (~120 m) in the section is dominated by black shales with subordinate dolostone. It is divided into four lithological members that can be roughly correlated with those in Yangtze Gorge area². More detailed information about the geological background and sample descriptions can be found in Supplementary Note 1. Three Ocean Oxygenation Events (OOEs) have previously been identified in this section (here termed intervals A, B, and C). They are characterized by increases in Mo/TOC and U/TOC ratios (Fig. 2), which indicates an increase in the marine reservoirs of Mo and U during these events². This inference is also partially supported by S-Mo-Tl-Cr isotopic variations in the same section (Supplementary Fig. 1). Importantly, the study site itself maintained anoxic and possibly sulfidic conditions, as it likely reflected a productive upwelling zone, akin to oxygen-minimum zones in the modern oxygenated ocean³⁰.

Various P phases including crystalline apatite P (mostly in the form of detrital P and then termed as P_{det}), iron-bounded P (P_{Fe}), authigenic P (P_{auth}), and organic-bound P (P_{org}) were sequentially extracted and analyzed (see Methods) following established protocols³¹. Detailed analyzed results are provided in Supplementary Table 1. The total P concentrations ($P_{tot} = P_{det} + P_{auth} + P_{Fe} + P_{org}$) exhibit a broad range (115–13164 ppm) in the Doushantuo Formation, with two prominent increases in the upper part of members II and III. This trend remains evident when normalized to Al contents (Fig. 2). In most of the samples, the major components of P_{tot} are P_{auth} (16–3229 ppm) and P_{det} (21–10395 ppm), with minor contribution from P_{Fe} (3–266 ppm) and P_{org} (<1–15 ppm) (Fig. 2). The ratios of organic carbon to organic P (C_{org}/P_{org}) are all markedly higher (>1500) than the Redfield ratio (106:1) (Fig. 2), while the ratios of organic carbon to reactive P (C_{org}/P_{react} , where P_{react} is defined as $P_{auth} + P_{Fe} + P_{org}$) scatter around the Redfield ratio. In OOE intervals, virtually all samples (except one from interval B) have C_{org}/P_{react} higher than 106:1. Conversely, most samples in the rest of section (termed as non-OOE intervals hereafter) have C_{org}/P_{react} lower or close to 106:1 (Fig. 2).

Discussion

Sediment phosphorus recycling is strongly linked to local redox conditions. Euxinic conditions are particularly conducive to sedimentary P release due to the formation of pyrite with much lower affinity to P than its precursor Fe

minerals and preferential release of organic-bound P during anaerobic remineralization of organic matter coupled with bacterial sulfate reduction^{11–13,32}. Iron speciation data indicate that the Doushantuo Formation in the Wuhe section was largely deposited in euxinic environments as most of samples display ratios of highly reactive iron (Fe_{HR}) to total iron (Fe_T) higher than 0.38 and ratios of pyrite iron (Fe_{PY}) to Fe_{HR} higher than 0.7 (Fig. 2; ref. 2). This observation is further supported by pyrite morphology³³. The exceptions are intervals A and B where variable Fe_{HR}/Fe_T and Fe_{PY}/Fe_{HR} values point to fluctuating redox conditions between euxinic, ferruginous ($Fe_{HR}/Fe_T > 0.38$; $Fe_{PY}/Fe_{HR} < 0.7$), and even sporadically oxic ($Fe_{HR}/Fe_T < 0.22$). Notwithstanding, the euxinic water mass may have expanded to the photic zone during intervals A, B, and C but shrunk to a narrow range in deep water areas during other times^{28,34}.

The well-constrained local redox conditions provide a framework for evaluating the extent of P recycling. The C_{org}/P_{org} ratios in our samples (average 15,755) are over two orders of magnitude higher than the average modern Redfield ratio and also higher than the ratio found in oligotrophic seawater of modern oceans (up to 600)³⁵. Comparable C_{org}/P_{org} values have been reported from the ca. 2.5 Ga Ghaap Group in South Africa³⁶, the ca. 650 Ma Datangpo/Xiangmeng Formation³⁷ and the ca. 520 Ma Mingxinsi Formation³⁸ in South China. The most resonable explanation for this observation is the preferential release of P_{org} relative to C_{org} during partially anaerobic remineralization of organic matter, as it is the only known original process capable of generating such extremely high C_{org}/P_{org} ^{12,36,37,39}. This inference is consistent with the Fe speciation data indicative of dominantly euxinic bottom water conditions³ and universally negative inorganic carbon isotope compositions ($\delta^{13}C_{carb}$) in the interlayered carbonates of the Wuhe section⁴⁰, all of which suggest an active microbial sulfate reduction, particularly conducive to preferential sedimentary P release.

The released P during organic matter remineralization can be recycled back into the water column to fuel primary productivity, or be trapped as authigenic phases in the sediment^{6,12–14}. To determine the fate of this released P and the magnitude of a potential benthic P flux from sediments back into the water column, we resort to the ratios of C_{org}/P_{react} as suggested, since reactive P represents potentially mobile P on early diagenetic timescales^{31,41}. However, this ratio could be elevated owing to the possible transfer of authigenic apatite to P_{det} during diagenesis (c.f. ref. 42). The C_{org}/P_{react} ratios in our samples show contrasting distribution patterns between OOE intervals and non-OOE intervals (Fig. 3). A one-tailed t-test indicates that the difference between the two groups is significant ($p = 0.016$). High C_{org}/P_{react} ratios relative to the modern Redfield ratio in OOE intervals could theoretically be caused by the conversion of authigenic apatite to P_{det} . This

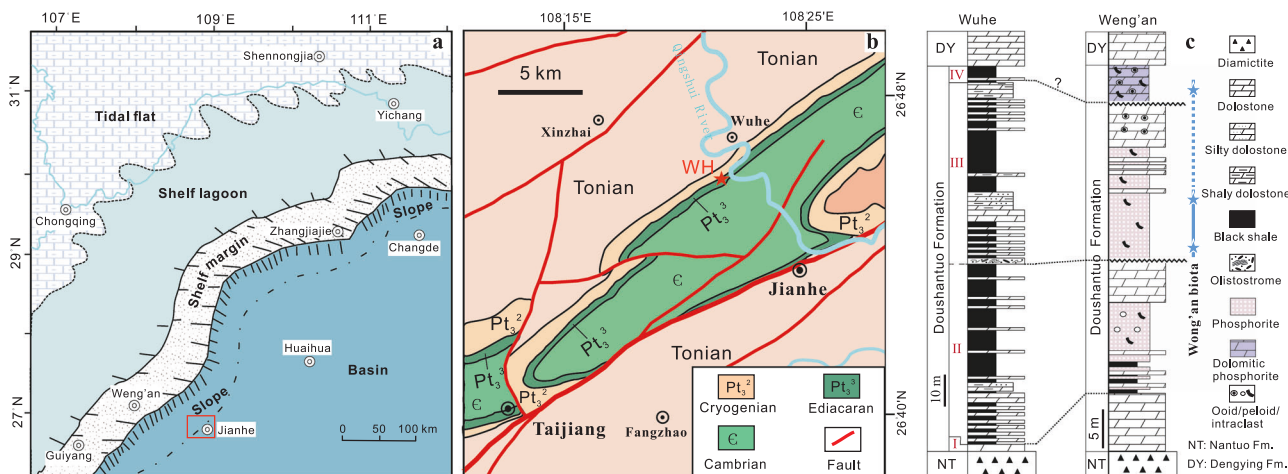


Fig. 1 | Location of study area and stratigraphic columns. **a** Generalized depositional model of South China during the Ediacaran Period (modified from ref. 59). **b** The geological map of the study area represented by the rectangle in (a). Red star marks the location of the Wuhe section investigated in this work. **c** Stratigraphic

correlation of Wuhe and Weng'an sections. The detailed information for age assignment in the Wuhe section is provided in Supplementary Fig. 1 and Note 1. The range of Weng'an biota refers to ref. 57.

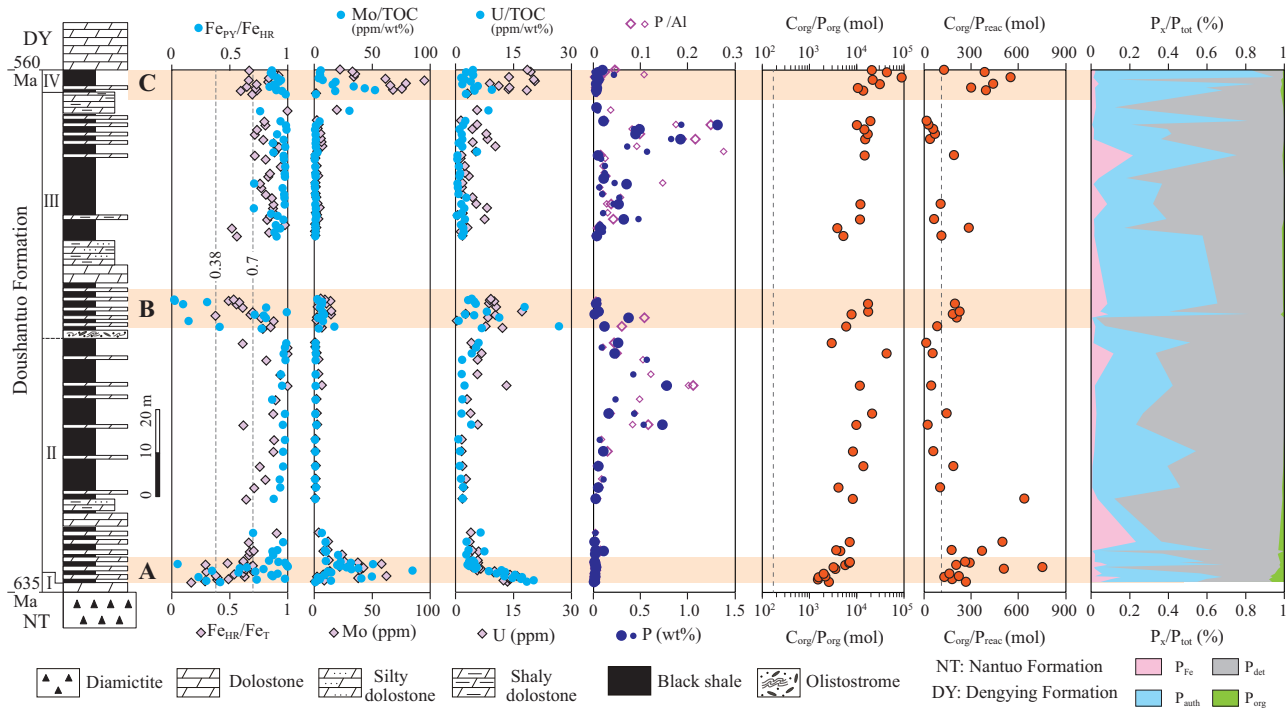


Fig. 2 | Stratigraphic distribution of Fe speciation, Mo, Mo/TOC, U, U/TOC, P, P/Al, and P phase partitioning. The Fe speciation, Mo, U, and P (small symbols) data are from ref. 2. The dashed lines in Fe speciation column indicate the cutoff values for anoxic ($Fe_{HR}/Fe_T > 0.38$) and euxinic ($Fe_{PY}/Fe_{HR} > 0.7$) conditions. The

dashed lines in C_{org}/P_{org} and C_{org}/P_{react} columns represent Redfield ratio (106:1). The horizontal bands (termed as A, B, and C) refer to the originally defined ocean oxygenation intervals based on strong enrichment of redox-sensitive elements.

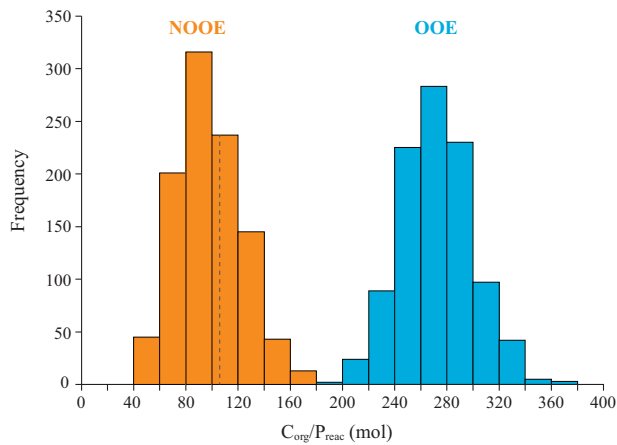


Fig. 3 | Frequency distributions of bootstrap resampled mean C_{org}/P_{react} ($n = 1000$) for the OOE and non-OOE intervals. The dashed line indicates the Redfield ratio (106:1). Note the contrasting distribution of the two groups.

interpretation is at odds with the strong positive correlation between P_{react} and P_{det} (Supplementary Fig. 2), because one would expect the opposite if this conversion were substantial. In addition, the average P_{det} are 92 ± 52 ppm, 162 ± 164 ppm, and 96 ± 58 ppm in intervals A, B, and C, respectively, which are similar, or lower than the concentrations that are typically observed in modern continental margins⁴³ (186 ± 21 ppm). On the contrary, the non-OOE intervals are featured by high P_{det} (2206 ± 2630 ppm) but low C_{org}/P_{react} . If this high P_{det} was caused by the conversion of P_{react} , the original C_{org}/P_{react} would have been much lower than the Redfield ratio. Given these considerations, potential recrystallization of authigenic apatite is unlikely to be the main cause for the variations of C_{org}/P_{react} in our samples. Sediment C_{org}/P_{tot} has also been used to investigate the extent of P remobilization during early diagenesis^{44–47}. However, the

addition of P_{det} in the calculation would inevitably underestimate the benthic P fluxes (lower C_{org}/P ratio) and lead to inaccurate estimates of P retention and regeneration, especially considering that P_{det} is the main component of P_{tot} in most fine-grained siliciclastic rocks^{37,38,41}.

A more reasonable explanation for the high C_{org}/P_{react} is therefore the enhanced release of recycled P back to water column, a situation similar to that documented in the Datangpo and Niutitang formations^{37,38}, the ca. 2.5 Ga Ghaap Group³⁶, and the ca. 2.93 Ga Red Lake sedimentary rock⁴⁸. In contrast, the low C_{org}/P_{react} values in the rest of the section can be attributed to retention of recycled P in the sediment through ‘sink switching’^{36,37,41}. In intervals A and B, the benthic P flux is evident (high C_{org}/P_{react}) in samples with varying redox conditions between ferruginous and euxinic inferred from Fe speciation (Fig. 2). The recycling is, however, largely suppressed in non-OOE interval samples with persistently euxinic conditions as evidenced by Fe speciation (Fig. 2). This seems counterintuitive, because sedimentary P release is generally more efficient in euxinic conditions due to bacterial sulfate reduction^{11–13,32}. We argue that this ‘unexpected’ outcome could be related to the change of concentration of pore water H_2S . Experimental work shows that the release of sedimentary P is positively correlated with the concentrations of pore water H_2S , with high H_2S (>0.6 mM) resulting in more P release and low H_2S favoring more P retention⁴⁹. Although it is difficult to precisely quantify the pore water H_2S concentrations during the deposition of the Doushantuo Formation, both pyrite sulfur isotope compositions ($\delta^{34}S_{PY}$) and mass-independent Hg isotopes ($\Delta^{199}Hg$) (Supplementary Fig. 1; ref. 2,28) from the Wuhe section suggest that seawater sulfate concentrations increased during OOE intervals but decreased in between, which could have led to the fluctuation of pore water H_2S . Alternatively, decreased upwelling during sea level lowstands²⁷ would have reduced the delivery of recycled P to the photic zone, which, to some degree, could increase the chance of their retention in sediments. However, current data do not allow us to distinguish between these two possibilities.

Multiple lines of geochemical evidence from the Wuhe section reveal several short-term OOE intervals during the Ediacaran^{2,3,23,27}. The OOE hypothesis

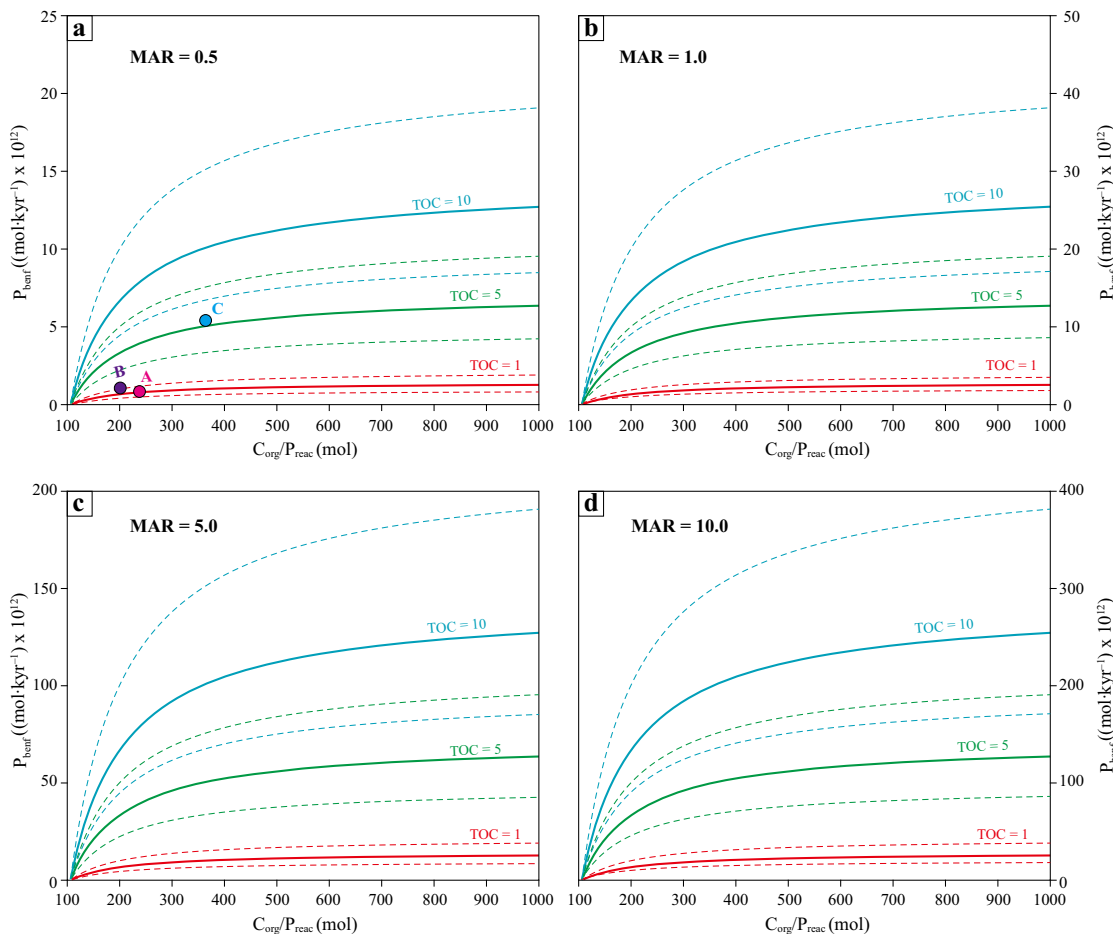


Fig. 4 | Model calculation of P_{benf} as a function of $C_{\text{org}}/P_{\text{reac}}$. Four panels display calculated P_{benf} results at different mass accumulation rate. **a** $0.5 \text{ g cm}^{-2} \text{ kyr}^{-1}$, **b** $1.0 \text{ g cm}^{-2} \text{ kyr}^{-1}$, **c** $5.0 \text{ g cm}^{-2} \text{ kyr}^{-1}$, and **d** $10.0 \text{ g cm}^{-2} \text{ kyr}^{-1}$. Different colors of lines refer to the results of different TOC contents. The solid lines represent modeled

results of 10% euxinic sediment, while the dashed lines indicate an increase and decrease of this value by a factor of 1.5. The filled circles in A indicate the modeled results for intervals A, B, and C.

has also been supported by evidence from other sections^{23,50–52}. Enhanced continental P input after the Marinoan Snowball was proposed as a main reason for elevated primary productivity and rising oxygen levels^{9,23}. This viewpoint is challenged by massive Ediacaran phosphorite deposition and stable median values of P content in mudstone from the Neoproterozoic to the early Paleozoic¹⁸. Alternatively, enhanced supply of recycled P was deemed as the main factor that resulted in high primary productivity, triggering OOE^{18,22,25,38}, though solid evidence was so far lacking. Our P speciation data provide sound evidence for this argument. In three highlighted intervals², high $C_{\text{org}}/P_{\text{reac}}$ ratios indicate efficient sedimentary P release to seawater, whereas low $C_{\text{org}}/P_{\text{reac}}$ ratios in the rest of the section imply limited P release.

We developed a mass balance model to quantify the contribution of the benthic P flux (P_{benf}) to primary productivity (see Model description in Methods). In this model, the benthic P flux is positively correlated with the sediment mass accumulation rate (MAR), TOC contents, and $C_{\text{org}}/P_{\text{reac}}$ ratios. With the updated age constraint assigned to the Wuhe section (Supplementary Fig. 1), the Doushantuo Formation is characterized by very slow MAR ($\sim 0.5 \text{ g cm}^{-2} \text{ kyr}^{-1}$). The TOC and $C_{\text{org}}/P_{\text{reac}}$ data were informed by our own analyses. Although TOC may vary among different sedimentary environments, the TOC contents from the Wuhe section are broadly consistent with the integrated TOC curve of this period⁵³. Admittedly, using data from only a single section could lead to some uncertainties for model results. Therefore, we also model a wide range of TOC and MAR (Fig. 4). Applying the average TOC and $C_{\text{org}}/P_{\text{reac}}$ values for the three OOE intervals and basic model parameters (Supplementary Table 2), the calculated P_{benf}

are $0.84 \times 10^{12} \text{ mol kyr}^{-1}$, $1.07 \times 10^{12} \text{ mol kyr}^{-1}$, and $5.41 \times 10^{12} \text{ mol kyr}^{-1}$ for intervals A, B, and C, respectively (Fig. 4a). Sensitivity tests using Monte Carlo simulations within 2 SD of TOC and $C_{\text{org}}/P_{\text{reac}}$ yield consistent results (Supplementary Fig. 3). Our estimation of P_{benf} during the intervals A and B is one order of magnitude lower than the proposed riverine P flux (including both dissolved and reactive P) during the Ediacaran (P_{in} , $\sim 5.0 \times 10^{13} \text{ mol kyr}^{-1}$, c.f. ref. 7); however, during interval C, P_{benf} reached up to $\sim 11\%$ of P_{in} indicating substantial contribution of benthic P to elevated seawater P levels and primary productivity. Notably, our model calculation may represent the most conservative results for the P_{benf} for the following reasons. First, we only consider a small portion of the total seafloor area in our model as we estimate that this would have been the area covered by productive euxinic margins (see Methods); second, MAR in the study section is likely much lower than the correlative strata on other continents⁵⁴. If we increased MAR to $10 \text{ g cm}^{-2} \text{ kyr}^{-1}$ (about 20 times higher than our estimate for the Doushantuo Formation), the calculated P_{benf} would be comparable to (for intervals A and B) or much higher (for interval C) than that of P_{in} (Fig. 4d).

Although the modeled P_{benf} for OOE intervals are all lower relative to P_{in} , they only account for a small portion of the total recycled P back to seawater. A large amount of recycled P would be released during the remineralization of organic matter in the water column before settling down to sediments or in porewater during early diagenesis. This water column recycling flux would have been particularly prominent in other parts of the ocean, where conditions were oxygenated during the OOE, i.e., away from the locally anoxic productive margin that characterizes our study site. It is

estimated that only ~8% of initial organic carbon was buried in the mid-Proterozoic, which is even less towards the Phanerozoic⁵⁵. Using 8% as a conservative estimate for the Ediacaran ocean, the total recycled P would reach up to 1.84×10^{13} mol kyr⁻¹ for interval A, 2.73×10^{13} mol kyr⁻¹ for interval B, and 9.31×10^{13} mol kyr⁻¹ for interval C. Therefore, the contribution of total recycled P to primary productivity in intervals A and B accounts for ~37% and ~67% of P_{ini} , while in interval C this contribution outpaced P_{ini} ⁷. For comparison, in the modern ocean, the riverine influx is very small (ca. 6.46×10^{10} mol per year) compared to the amount that is used by primary producers in the photic zone (ca. 38.74×10^{12} mol per year)⁵⁶, and this discrepancy is enabled by highly efficient P recycling in the modern oxygenated water column. Importantly, we are not proposing that the P cycle deviates from steady state, whereafter total P input by weathering equals total P burial in sediments. Instead, enhanced recycling would simply have increased the residence time of P in the water column. The enhancement of P regeneration may have been initiated by increased sulfate supply from continental weathering. The coupled bacterial sulfate reduction and organic matter remineralization along productive continental margins, such as our study site, would have enhanced the recycled P flux from sediments, promoting primary productivity and organic matter burial, and accordingly short-term oxygenation events as recorded during the Ediacaran²⁴. Elevated seawater P and ensuing ocean oxygenation may have stimulated animal evolution, as documented in the Weng'an biota⁵⁷ (Fig. 1c). Ultimately, the expansion of oxic P sinks and consumption of O₂ by a high organic matter load may have led to the return of widespread anoxia outside of OOE.

The P speciation data presented here can also explain the spatio-temporal distribution of massive Ediacaran phosphorite⁵⁸. Three phosphorite layers were recorded in the Doushantuo Formation in shallow-water sections. Integrated stratigraphic correlations suggest that these phosphorite layers were broadly coeval with the OOE intervals⁵⁹ (Fig. 1; Supplementary Note 2). We argue that upwelling of recycled P brought excessive nutrients to the shallow shelf where phosphorites formed under favorable conditions, as recorded in their modern analogues⁶⁰.

In summary, our P speciation data and mass balance calculation provide important insights into the Ediacaran P cycle and its linkage to ocean redox change. High C_{org}/P_{org} and C_{org}/P_{reac} ratios relative to the Redfield ratio imply the efficient release of P back to the water column in these purported OOE intervals. Conversely, high C_{org}/P_{org} but low C_{org}/P_{reac} ratios in between suggest a retention of recycled P in sediments. Mass balance calculations indicate that the contribution of recycled P to primary productivity could be comparable to or outpace that of weathering P input. This work supports the hypothesis that P recycling may have played an important role in elevated seawater P concentrations, increased organic matter burial and subsequently Ediacaran OOE, which, in turn, facilitated the rapid diversification of animals during this critical period. A similar mechanism has also been proposed for other oxygenation events or oxygen oases in the Precambrian and early Cambrian^{36–58,48}, providing confidence in the importance of regional euxinia in driving the global P cycle.

Methods

Phosphorus speciation

Chemical procedures and measurements for P speciation are conducted in the University of Science and Technology of China following the methods referring to a modified SEDEX method³¹. Six operationally-defined phosphorus pools were targeted, including Fe (oxyhydr)oxide-bound P (P_{Fe1}), authigenic carbonate fluorapatite-associated P (P_{auth}), crystalline apatite (mostly in the form of detrital P_{det}), magnetite-bound P (P_{mag}), crystalline Fe-bound P (P_{Fe2}), and organic P (P_{org}), extracted using different reagents. Approximately 150 mg powder of each sample is weighed in a 15 ml centrifuge tube with 10 ml dithionite-citrate-bicarbonate solution (mixture of 0.3 M sodium citrate, 1 M sodium bicarbonate and 0.15 M sodium dithionite, pH = 7.6) and shaken for 8 h at room temperature. After centrifugation, the residue is cleaned up using 10 ml 1 M MgCl₂ (pH = 8, NaOH buffered, same as below) and ultra-pure water (resistivity > 18.2 MΩ cm) for twice times. Wherein the supernatants are collected to measure P_{Fe1}

concentrations. Subsequently, 10 mL 1M NaAc (pH = 4, HAc buffered) is added to the residue and shaken for 6 h at room temperature. After centrifugation, the residue is washed twice with 10 ml 1 M MgCl₂, then rinsed by ultra-pure water. The supernatants of this step are collected for P_{auth} concentration measurement. The residue is then mixed with 10 ml 1 M HCl and shaken for 16 h, while the supernatant is analyzed for P_{det} concentration. After being rinsed with ultra-pure water, the residue is treated with 10 ml ammonium oxalate for 6 h. Following centrifugation, the residue is cleaned up using 10 ml ultra-pure water twice. The supernatants of this step are used to measure for P_{mag} concentration. The residue was then added with 10 ml mixture of 0.3 M sodium dithionite and 0.2 M sodium citrate (pH = 4.8, HAc buffered) and shaken for 6 h. After centrifugation, the residue is washed with 10 ml ultra-pure water twice. The supernatants of this step are used to measure for P_{Fe2} concentration. The residue then transfers to a ceramic crucible and is ashed at 550 °C for 2 h. The ashed powder is added with 1 M HCl in a 15 ml centrifuge tube for 16 h, then centrifuged. The supernatants of this step are measured for P_{org} concentration. For all extracted phosphorus, it is measured by ICP-OES (SPECTRO ARCOS III). Replicate analysis of a sample gave a relative standard deviation of <10% for each step, except for P_{Fe} because of the low concentrations.

Model description

We developed a mass balance model to quantitatively determine the benthic phosphorus flux (P_{benf} unit in mol kyr⁻¹) to evaluate the relative contribution of recycled P to primary productivity in the Ediacaran ocean. In steady state, P_{benf} can be calculated using the following equation:

$$P_{benf} = P_{ini} - P_{rem} \quad (1)$$

where P_{ini} refers to the amount of initial P in the sediments during deposition, and P_{rem} represents the amount of P remaining in sedimentary rocks. Assuming (1) the initial sediment C_{org}:P remains the same as the Redfield ratio (106:1), and (2) the reduction of TOC contents due to decomposition in sediment were limited after precipitation, the P_{ini} and P_{rem} can be approximated using the following two equations:

$$TOC_{tbf} : P_{ini} = 106 : 1 \quad (2)$$

$$TOC_{tbf} : P_{rem} = C_{org} : P_{reac} \quad (3)$$

The subscript 'tbf' in TOC refers to total burial flux (unit in mol kyr⁻¹) in the global ocean. For simplicity, TOC_{tbf} can be estimated as the product of organic carbon accumulation rate (OCAR) and area of seafloor (A_{sf}). OCAR is mainly dependent on the export flux of organic matter (sediment TOC contents were used as a proxy of export flux in our model, despite some or even most of them would be remineralized after deposition) and the MAR of sediment, both of which varied in different oceanic settings. To avoid this uncertainty, we only consider the euxinic continental margin sediments. The area of euxinic sediment is not well constrained. Previous Fe speciation and $\Delta^{199}\text{Hg}$ data suggested expanded euxinic environments from the lower slope to the photic zone^{28,33}, which may cover a large area of continental margin settings. In modern oceans, continental margins account for ~17% of global seafloor area⁶¹. We use an estimate of 10% euxinic sediment in our calculation. We also performed a simulation when this value is increased and decreased by a factor of 1.5. Therefore, TOC_{tbf} can be expressed as:

$$TOC_{tbf} = OCAR * A_{sf} * 10\% \quad (4)$$

and

$$OCAR = MAR * TOC \quad (5)$$

Applying a typical density for sedimentary rocks (2.5 g cm⁻³), MAR can be readily calculated if the ages of sedimentary rocks can be well

constrained. Merging the latter four equations into formula (1), we can model the P_{benf} as function of $C_{\text{org}} \cdot P_{\text{reac}}$.

Reporting summary

Further information on research design is available in the Nature Portfolio Reporting Summary linked to this article.

Data availability

All data reported in this paper can be accessed in the Supplementary Information and are also available at figshare repository: <https://doi.org/10.6084/m9.figshare.29206409>.

Received: 9 February 2025; Accepted: 9 June 2025;

Published online: 20 June 2025

References

- Li, C., Cheng, M., Zhu, M. & Lyons, T. W. Heterogeneous and dynamic marine shelf oxygenation and coupled early animal evolution. *Emerg. Top. Life Sci.* **2**, 279–288 (2018).
- Sahoo, S. K. et al. Oceanic oxygenation events in the anoxic Ediacaran ocean. *Geobiology* **14**, 457–468 (2016).
- Xu, D. et al. Chromium isotope evidence for oxygenation events in the Ediacaran ocean. *Geochim. Cosmochim. Acta* **323**, 258–275 (2022).
- Xiao, S. et al. Towards an ediacaran time scale: Problems, protocols, and prospects. *Episodes* **39**, 540–555 (2016).
- Tyrrell, T. The relative influences of nitrogen and phosphorus on oceanic primary production. *Nature* **400**, 525–531 (1999).
- Ruttenberg, K. C. The global phosphorus cycle. Treatise on geochemistry: 2nd edn, vol. 10 (Elsevier Ltd., 2014).
- Zhao, M. et al. Drivers of the global phosphorus cycle over geological time. *Nat. Rev. Earth Environ.* **5**, 873–889 (2024).
- Cox, G. M. et al. Continental flood basalt weathering as a trigger for Neoproterozoic Snowball Earth. *Earth Planet. Sci. Lett.* **446**, 89–99 (2016).
- Planavsky, N. J. et al. The evolution of the marine phosphate reservoir. *Nature* **467**, 1088–1090 (2010).
- Squire, R. J., Campbell, I. H., Allen, C. M. & Wilson, C. J. L. Did the Transgondwanan Supermountain trigger the explosive radiation of animals on Earth? *Earth Planet. Sci. Lett.* **250**, 116–133 (2006).
- Ingall, E. D., Bustin, R. M. & Van Cappellen, P. Influence of water column anoxia and sediment supply on the burial and preservation of organic carbon in marine shales. *Geochim. Cosmochim. Acta* **57**, 303–316 (1993).
- Ingall, E. & Jahnke, R. Evidence for enhanced phosphorus regeneration from marine sediments overlain by oxygen depleted waters. *Geochim. Cosmochim. Acta* **58**, 2571–2575 (1994).
- Van Cappellen, P. & Ingall, E. D. Benthic phosphorus regeneration, net primary production, and ocean anoxia: a model of the coupled marine biogeochemical cycles of carbon and phosphorus. *Paleoceanography* **9**, 677–692 (1994).
- Xiong, Y. et al. Phosphorus cycling in Lake Cadagno, Switzerland: a low sulfate euxinic ocean analogue. *Geochim. Cosmochim. Acta* **251**, 116–135 (2019).
- Slomp, C. P. et al. Coupled dynamics of iron and phosphorus in sediments of an oligotrophic coastal basin and the impact of anaerobic oxidation of methane. *PLoS ONE* **8**, e62386 (2013).
- Cosmidis, J. et al. Biomineralization of iron-phosphates in the water column of Lake Pavin (Massif Central, France). *Geochim. Cosmochim. Acta* **126**, 78–96 (2014).
- Egger, M., Jilbert, T., Behrends, T., Rivard, C. & Slomp, C. P. Vivianite is a major sink for phosphorus in methanogenic coastal surface sediments. *Geochim. Cosmochim. Acta* **169**, 217–235 (2015).
- Laakso, T. A., Sperling, E. A., Johnston, D. T. & Knoll, A. H. Ediacaran reorganization of the marine phosphorus cycle. *Proc. Natl. Acad. Sci. USA* **117**, 11961–11967 (2020).
- Reinhard, C. T. et al. Evolution of the global phosphorus cycle. *Nature* **541**, 386–389 (2017).
- Planavsky, N. J. et al. A sedimentary record of the evolution of the global marine phosphorus cycle. *Geobiology* **21**, 168–174 (2023).
- Yang, X. et al. A phosphate-rich marine reservoir in the redox stratified Ediacaran ocean. *Commun. Earth Environ.* **5**, 41 (2024).
- Dodd, M. S. et al. Uncovering the Ediacaran phosphorus cycle. *Nature* **618**, 974–980 (2023).
- Sahoo, S. K. et al. Ocean oxygenation in the wake of the Marinoan glaciation. *Nature* **489**, 546–549 (2012).
- Alcott, L. J., Mills, B. J. W. & Poulton, S. W. Stepwise Earth oxygenation is an inherent property of global biogeochemical cycling. *Science* **366**, 1333–1337 (2019).
- Fan, H. et al. Phosphorus flux during the Ediacaran: Rooted in continental weathering or pelagic upwelling?. *Earth Planet. Sci. Lett.* **646**, 118975 (2024).
- Kipp, M. A. & Stüeken, E. E. Biomass recycling and Earth's early phosphorus cycle. *Sci. Adv.* **3**, eaao4795 (2017).
- Ostrander, C. M. et al. Multiple negative molybdenum isotope excursions in the Doushantuo Formation (South China) fingerprint complex redox-related processes in the Ediacaran Nanhua Basin. *Geochim. Cosmochim. Acta* **261**, 191–209 (2019).
- Zheng, W. et al. Recurrent photic zone euxinia limited ocean oxygenation and animal evolution during the Ediacaran. *Nat. Commun.* **14**, 3920 (2023).
- Zhang, S. et al. New paleomagnetic results from the Ediacaran Doushantuo Formation in South China and their paleogeographic implications. *Precambrian Res.* **259**, 130–142 (2015).
- Scholz, F. Identifying oxygen minimum zone-type biogeochemical cycling in Earth history using inorganic geochemical proxies. *Earth Sci. Rev.* **184**, 29–45 (2018).
- Thompson, J. et al. Development of a modified SEDEX phosphorus speciation method for ancient rocks and modern iron-rich sediments. *Chem. Geol.* **524**, 383–393 (2019).
- Slomp, C. P., Thomson, J. & De Lange, G. J. Controls on phosphorus regeneration and burial during formation of eastern Mediterranean sapropels. *Mar. Geol.* **203**, 141–159 (2004).
- Wang, L., Shi, X. & Jiang, G. Pyrite morphology and redox fluctuations recorded in the Ediacaran Doushantuo Formation. *Palaeogeogr. Palaeoclimatol. Palaeoecol.* **333**, 218–227 (2012).
- Li, C. et al. A stratified redox model for the ediacaran ocean. *Science* **328**, 80–83 (2010).
- Teng, Y. C., Primeau, F. W., Moore, J. K., Lomas, M. W. & Martiny, A. C. Global-scale variations of the ratios of carbon to phosphorus in exported marine organic matter. *Nat. Geosci.* **7**, 895–898 (2014).
- Alcott, L. J., Mills, B. J. W., Bekker, A. & Poulton, S. W. Earth's great oxidation event facilitated by the rise of sedimentary phosphorus recycling. *Nat. Geosci.* **15**, 210–215 (2022).
- Bowyer, F. T. et al. Biological diversification linked to environmental stabilization following the Sturtian Snowball glaciation. *Sci. Adv.* **9**, eadff999 (2023).
- Liu, Y. et al. Marine redox and nutrient dynamics linked to the Cambrian radiation of animals. *Geology* **52**, 729–734 (2024).
- Steenbergh, A. K., Bodelier, P. L. E., Hoogveld, H. L., Slomp, C. P. & Laanbroek, H. J. Phosphatases relieve carbon limitation of microbial activity in Baltic Sea sediments along a redox-gradient. *Limnol. Oceanogr.* **56**, 2018–2026 (2011).
- Jiang, G. Q., Zhang, S. H., Shi, X. Y. & Wang, X. Q. Chemocline instability and isotope variations of the Ediacaran Doushantuo basin in South China. *Sci. China, Ser. D. Earth Sci.* **51**, 1560–1569 (2008).
- Guilbaud, R. et al. Phosphorus-limited conditions in the early Neoproterozoic ocean maintained low levels of atmospheric oxygen. *Nat. Geosci.* **13**, 296–301 (2020).
- Creveling, J. R. et al. Phosphorus sources for phosphatic Cambrian carbonates. *Bull. Geol. Soc. Am.* **126**, 145–163 (2014).

43. Ruttenberg, K. C. & Berner, R. A. Authigenic apatite formation and burial in sediments from non-upwelling, continental margin environments. *Geochim. Cosmochim. Acta* **57**, 991–1007 (1993).
44. Algeo, T. J. & Ingall, E. Sedimentary Corg:P ratios, paleocean ventilation, and Phanerozoic atmospheric pO₂. *Palaeogeogr. Palaeoclimatol. Palaeoecol.* **256**, 130–155 (2007).
45. Kraal, P., Slomp, C. P., Forster, A., Kuypers, M. M. M. & Sluijs, A. Pyrite oxidation during sample storage determines phosphorus fractionation in carbonate-poor anoxic sediments. *Geochim. Cosmochim. Acta* **73**, 3277–3290 (2009).
46. Kraal, P., Slomp, C. P., Forster, A. & Kuypers, M. M. M. Phosphorus cycling from the margin to abyssal depths in the proto-Atlantic during oceanic anoxic event 2. *Palaeogeogr. Palaeoclimatol. Palaeoecol.* **295**, 42–54 (2010).
47. Papadomanolaki, N. M., Lenstra, W. K., Wolthers, M. & Slomp, C. P. Enhanced phosphorus recycling during past oceanic anoxia amplified by low rates of apatite authigenesis. *Sci. Adv.* **8**, eabn2370 (2022).
48. Cañadas, F. et al. Archaean oxygen oases driven by pulses of enhanced phosphorus recycling in the ocean. *Nat. Geosci.* **18**, 430–435 (2025).
49. Kubeneck, L. J. et al. Transformation of vivianite in intertidal sediments with contrasting sulfide conditions. *Geochim. Cosmochim. Acta* **370**, 173–187 (2024).
50. Scott, C. et al. Tracing the stepwise oxygenation of the Proterozoic ocean. *Nature* **452**, 456–459 (2008).
51. Och, L. M. et al. Palaeoceanographic controls on spatial redox distribution over the yangtze platform during the Ediacaran–Cambrian transition. *Sedimentology* **63**, 378–410 (2016).
52. Yuan, L. et al. Multiple ocean oxygenation events during the Ediacaran Period: Mo isotope evidence from the Nanhua Basin, South China. *Precambrian Res.* **388**, 107004 (2023).
53. Wei, G. Y. et al. Lithium isotopic constraints on the evolution of continental clay mineral factory and marine oxygenation in the earliest Paleozoic Era. *Sci. Adv.* **10**, eadk2152 (2024).
54. Miller, A. J. et al. Tracking the onset of Phanerozoic-style redox-sensitive trace metal enrichments: New results from basal Ediacaran post-glacial strata in NW Canada. *Chem. Geol.* **457**, 24–37 (2017).
55. Planavsky, N. J. et al. on Carbon Burial and Net Primary Production Through Earth'S History. *Am. J. Sci.* **322**, 413–460 (2022).
56. Schlesinger W. H. & Bernhardt, E. S. Biogeochemistry: an analysis of global change: Third Edition (Academic Press, 2013).
57. Xiao, S. et al. The Weng'an biota and the Ediacaran radiation of multicellular eukaryotes. *Natl. Sci. Rev.* **1**, 498–520 (2014).
58. Zhang, Y. et al. Economic phosphorite from the Ediacaran Doushantuo Formation, South China, and the Neoproterozoic-Cambrian Phosphogenic Event. *Sediment. Geol.* **388**, 1–19 (2019).
59. Jiang, G., Shi, X., Zhang, S., Wang, Y. & Xiao, S. Stratigraphy and paleogeography of the Ediacaran Doushantuo Formation (ca. 635–551Ma) in South China. *Gondwana Res.* **19**, 831–849 (2011).
60. Föllmi, K. B. The phosphorus cycle, phosphogenesis and marine phosphate-rich deposits. *Earth Sci. Rev.* **40**, 55–124 (1996).
61. Cogley, J. G. Continental margins and the extent and number of the continents. *Rev. Geophys.* **22**, 101–122 (1984).

Acknowledgements

This study was supported by the National Natural Science Foundation of China (41930320), the Chinese 111 project (B20011), the Deep-time Digital Earth Science and Technology Leading Talents Team Funds for the Central Universities for the Frontiers Science Center for Deep-time Digital Earth, China University of Geosciences (Beijing) (2652023001). No permissions were required for sampling. We thank Yafang Song for her assistance in P speciation analyses. We are grateful to three anonymous reviewers for the constructive comments that improved the paper.

Author contributions

X.W., J.H., and X.S. designed the research. D.X., W.X., and Z.Q. performed P analyses. X.W. and E.S. developed the mass balance model. All authors contributed to data interpretation. X.W., D.X., and X.S. wrote the manuscript with contributions from E.S., W.X., Z.Q., J.H., and D.T.

Competing interests

The authors declare no competing interests.

Additional information

Supplementary information The online version contains supplementary material available at <https://doi.org/10.1038/s43247-025-02463-2>.

Correspondence and requests for materials should be addressed to Xinqiang Wang.

Peer review information *Communications Earth and Environment* thanks Mingyu Zhao and the other, anonymous, reviewer(s) for their contribution to the peer review of this work. Primary Handling Editors: Feifei Zhang and Alice Drinkwater. [A peer review file is available].

Reprints and permissions information is available at <http://www.nature.com/reprints>

Publisher's note Springer Nature remains neutral with regard to jurisdictional claims in published maps and institutional affiliations.

Open Access This article is licensed under a Creative Commons Attribution 4.0 International License, which permits use, sharing, adaptation, distribution and reproduction in any medium or format, as long as you give appropriate credit to the original author(s) and the source, provide a link to the Creative Commons licence, and indicate if changes were made. The images or other third party material in this article are included in the article's Creative Commons licence, unless indicated otherwise in a credit line to the material. If material is not included in the article's Creative Commons licence and your intended use is not permitted by statutory regulation or exceeds the permitted use, you will need to obtain permission directly from the copyright holder. To view a copy of this licence, visit <http://creativecommons.org/licenses/by/4.0/>.

© The Author(s) 2025